

Tilt and decentration of intraocular lenses in vivo from Purkinje and Scheimpflug imaging

Validation study

Alberto de Castro, BSc, Patricia Rosales, MSc, Susana Marcos, PhD

PURPOSE: To measure tilt and decentration of intraocular lenses (IOLs) with Scheimpflug and Purkinje imaging systems in physical model eyes with known amounts of tilt and decentration and patients.

SETTING: Instituto de Óptica Daza de Valdés, Consejo Superior de Investigaciones Científicas, Madrid, Spain.

METHODS: Measurements of IOL tilt and decentration were obtained using a commercial Scheimpflug system (Pentacam, Oculus), custom algorithms, and a custom-built Purkinje imaging apparatus. Twenty-five Scheimpflug images of the anterior segment of the eye were obtained at different meridians. Custom algorithms were used to process the images (correction of geometrical distortion, edge detection, and curve fittings). Intraocular lens tilt and decentration were estimated by fitting sinusoidal functions to the projections of the pupillary axis and IOL axis in each image. The Purkinje imaging system captures pupil images showing reflections of light from the anterior corneal surface and anterior and posterior lens surfaces. Custom algorithms were used to detect the Purkinje image locations and estimate IOL tilt and decentration based on a linear system equation and computer eye models with individual biometry. Both methods were validated with a physical model eye in which IOL tilt and decentration can be set nominally. Twenty-one eyes of 12 patients with IOLs were measured with both systems.

RESULTS: Measurements of the physical model eye showed an absolute discrepancy between nominal and measured values of 0.279 degree (Purkinje) and 0.243 degree (Scheimpflug) for tilt and 0.094 mm (Purkinje) and 0.228 mm (Scheimpflug) for decentration. In patients, the mean tilt was less than 2.6 degrees and the mean decentration less than 0.4 mm. Both techniques showed mirror symmetry between right eyes and left eyes for tilt around the vertical axis and for decentration in the horizontal axis.

CONCLUSIONS: Both systems showed high reproducibility. Validation experiments on physical model eyes showed slightly higher accuracy with the Purkinje method than the Scheimpflug imaging method. Horizontal measurements of patients with both techniques were highly correlated. The IOLs tended to be tilted and decentered nasally in most patients.

J Cataract Refract Surg 2007; 33:418–429 © 2007 ASCRS and ESCRS

In the past few years, cataract surgery has benefited significantly from technological advances. While eliminating the intraocular diffusion produced by the cataract is still the reason for the procedure, advances in optical measurements and intraocular lens (IOL) design provide good refractive outcomes and even aim at canceling the spherical aberration of the cornea. In addition to monofocal IOLs, advances have also been made in multifocal and pseudoaccommodating IOL

design.^{1,2} Concern about surgically induced aberrations, initially limited to refractive surgery,³ is also present in cataract procedures.⁴

Measurements of the ocular and total aberrations after cataract surgery show higher spherical aberrations in eyes with monofocal spherical IOLs.⁵ Recent designs with aspherical surfaces induce negative spherical aberration, with the aim of mimicking that of the young crystalline lens.⁶ There are even

proposals for IOLs aiming to cancel other higher-order aberrations.⁷

The ultimate limitation of the customized IOL is precision in its positioning. There have been theoretical studies of the impact of IOL tilt and decentration on optical quality with new aspherical lenses.^{6,8} In a previous study,⁴ we also assessed this question *in vitro* for spherical lenses and suggest that the effect of IOL tilt and decentration in the final optical quality depends greatly on the actual combination of tilt and decentration in an eye. Therefore, individually measuring tilt and decentration 3-dimensionally is important to assess the optical degradation imposed by IOL positioning and evaluate the benefits of specific designs implanted in real eyes.

Two methods have been used to measure IOL tilt and decentration *in vivo*: Purkinje imaging and Scheimpflug imaging. Purkinje images are reflections from the anterior (PI) and posterior (PII, usually not visible) corneal surfaces and from the anterior (PIII) and posterior (PIV) lens surfaces. Since their description by Purkinje in 1832, the images have been used to measure cornea and crystalline properties, particularly phakometry. Clinical studies report the use of Purkinje images to obtain biometric data^{9,10} or to assess IOL tilt and decentration.¹¹ A more systematic approach is that proposed by Phillips et al.¹² and then further used by Barry et al.¹³ These authors propose a set of linear equations relating the position of PI, PIII, and PIV as a function of linear combinations of eye rotation, IOL tilt, and IOL decentration. In addition, they incorporated a telecentric IOL to avoid parallax because PIII lies on a different focal plane. Based on these concepts, our laboratory developed a compact system to measure phakometry and crystalline lens tilt and decentration.¹⁴ The system has been extensively validated both computationally and experimentally.^{14,15}

Accepted for publication October 29, 2006.

From the Instituto de Óptica Daza de Valdés, Consejo Superior de Investigaciones Científicas, Madrid, Spain.

No author has a financial or proprietary interest in any material or method mentioned.

Supported by grant #FIS2005-04382 from the Ministerio de Educación y Ciencia and an European Young Investigator Award (EURHORCs) to Dr. Marcos.

Sergio Ortiz, MSc, Jose Requejo-Isidro, PhD, and Ignacio Jiménez-Alfaro, MD, PhD, supplied technical assistance and helpful discussions.

Corresponding author: Alberto de Castro, Instituto de Optica Daza de Valdes, CSIC, Serrano 121, Madrid-28006, Spain. E-mail: alberto@io.cfmac.csic.es.

The Scheimpflug camera provides images of the anterior chamber of the eye. Its configuration is such that the image, lens, and object plane intersect in 1 point so that sections of the eye appear with large depth of focus. Conversely, Scheimpflug images suffer from geometric distortion (resulting from tilt of the object, lens, and image planes) and optical distortion (because the different surfaces are viewed through anterior refracting surfaces). Ray-tracing techniques are therefore required to obtain reliable crystalline surface geometry.^{16,17} Scheimpflug research instruments¹⁸⁻²⁰ have been used to study the shape of the crystalline lens and how it changes with accommodation or aging.^{16,20} Phakometry data from Scheimpflug imaging have been compared with data from other techniques. Koretz et al.²¹ compared the anterior and posterior radii of curvature from the Scheimpflug technique with those measured by magnetic resonance imaging in 2 sets of subjects as a function of age. In a previous study,¹⁵ we compared anterior and posterior radii of curvature obtained with Scheimpflug and Purkinje imaging in the same group of eyes, both unaccommodated and as a function of accommodation in a subset of eyes. The clinical literature includes numerous reports of IOL tilt and decentration at different times after surgery or with different IOL types using commercial Scheimpflug instruments.²²⁻²⁸ With these instruments, the optical distortion is presumably not corrected. Only a recent study of IOL tilt and decentration in eyes with phakic lenses²⁹ using a Nidek Scheimpflug system mentions that images were corrected using custom algorithms.

The availability of new Scheimpflug commercial instruments may make the measurement of IOL tilt and decentration more accessible. However, powerful data-processing routines, careful assessment of the limitations of the technique, and experimental validations are necessary before this information can be used reliably.

In this manuscript, we present measurements of IOL tilt and decentration of IOLs in a water-cell model eye and in patients using a custom Purkinje imaging system and Pentacam Scheimpflug imaging with custom algorithms. To our knowledge, this is the first assessment of the accuracy of the techniques in measuring IOL tilt and decentration and the first cross-validation of Scheimpflug and Purkinje imaging to measure tilt and decentration.

MATERIALS AND METHODS

Purkinje imaging system

A system for phakometry and lens tilt and decentration measurements based on phakometry and

implemented at the Instituto de Optica, Consejo Superior de Investigaciones Científicas, was used in the study. The optical setup, processing algorithms, and validations have been described.¹⁴ In brief, the system consists of (1) 2 illuminating channels (for measurements in right eyes and left eyes) with collimated light from infrared (IR) light-emitting diodes (LEDs) at an angle of 12 degrees horizontally; (2) an imaging channel with an IR-enhanced charge-coupled device (CCD) camera with a telecentric lens mounted in front of the eye and conjugate with the eye's pupil; (3) a fixation channel with a minidisplay, collimating lens, and Badal system that allows projection of visual stimuli foveally and at different eccentricities, as well as correction of refraction. The system sits on a 500 mm × 400 mm optical table. Software written in Visual Basic (Microsoft Visual Studio 6.0) automatically controls the image acquisition, LED switching, and stimulus display. Data processing is performed using Matlab (Mathworks, Inc.) and the Zemax optical design program (Focus Software). The detection of Purkinje images PI, PII, and PIII and the pupil center in the pupil images is performed using Gaussian fitting with routines written in Matlab. The processing routines assume that P1, P3, and P4 (positions of PI, PII and PIII, respectively, relative to the center of the pupil) are linearly related to eye rotation (β), lens tilt (α), and lens decentration (d).

$$P1 = E\beta$$

$$P3 = F\beta + A\alpha + Cd$$

$$P4 = G\beta + B\alpha + Dd$$

These equations are applied to both horizontal and vertical coordinates. Coefficients A through G are obtained using a computer model eye (simulated using biometric data available for each eye). Intraocular lens decentration is referred to the pupil center, and IOL tilt is referred to the pupillary axis. Computer simulations using realistic eye models and the actual specifications of the experimental setup showed maximum discrepancies between nominal and experimental values of 0.1 degree for eye rotation, 0.25 degree for IOL tilt, and 0.013 mm for IOL decentration.

Scheimpflug imaging

A commercial Scheimpflug imaging System (Pentacam, Oculus) was used to image sections of the anterior segment of the eye at different meridians (25) by projecting a slit (blue light). The systems' software corrects geometric distortion but shows uncorrected images. Because work was performed directly on the images captured, a routine was implemented to

correct this distortion. The commercial software provides quantitative information about the anterior and posterior corneal surfaces, but not the crystalline lens or IOL. In addition, the edge detection routines usually fail to detect the edges of certain types of IOLs (ie, acrylic) because their scattering properties are different from those of the crystalline lens. Algorithms that work directly on the raw images and calculate IOL tilt and decentration were developed. These include the following:

1. *Correction of the geometrical distortion of the images.* The appropriate correction was found with previous calibrations using a reticule.
2. *Routines to find the edges of the cornea and IOLs.* Two approaches are used depending on the diffusing properties of the IOLs (threshold filtering and edge detection of binary images for the crystalline lens and more diffusing lenses and detection of maximum values at the edge of the lens for the least diffusing lenses).
3. *Routines fitting the edges of the pupil and lens to find the pupil center, IOL center, IOL tilt, and eye rotation.* The pupil center is calculated as the midpoint between the 2 visible pupil segments. The IOL center is calculated as the midpoint of the intersection of the 2 circumferences that fit the anterior and posterior edges of the IOL. The reference axis is calculated as the line passing through the anterior corneal center of curvature and the center of the pupil, known as the pupillary axis.³⁰ The IOL axis (**L**) is calculated as the line joining the centers of curvature of the anterior and posterior lens edges. These axes are referred to a vertical axis in each image.
4. *Application of these procedures to each of the 25 sections obtained at each meridian.* For each meridian, the calculated parameters are projected to the horizontal and vertical axes. These projections (as a function of meridian angle) are fitted to a sinusoidal function. The horizontal and vertical components of pupil center, IOL center, IOL axis, and pupillary axis are then computed, evaluating the fitted sinusoidal functions at 90 degrees and 180 degrees.
5. *Intraocular lens decentration is obtained from the distance between the IOL center and the pupillary axis.* A scale of 0.02 mm/pixel in the lateral dimension was used. This factor was obtained in the calibration process described in number 1 above after the geometric distortion was corrected using the same reticule. Because there were no optical surfaces in the object, optical distortion does not influence this scale factor. The angles between axes are obtained by means of scalar products. The angle between the pupillary axis **P** and the line of sight (λ) is

calculated directly from the components of the pupillary axis as follows:

$$\cos\lambda_x = \frac{P_z \times \Delta z}{\sqrt{P_y^2 + P_z^2} \times \sqrt{\Delta z^2}}$$

$$\cos\lambda_y = \frac{P_x \times \Delta z}{\sqrt{P_x^2 + P_z^2} \times \sqrt{\Delta z^2}}$$

The angle between the lens axis L and the reference axis P (α) is obtained by means of the scalar product of the 2 director vectors.

$$\cos\alpha_x = \frac{P_y \times I_y + \Delta z \times \Delta z}{\sqrt{P_y^2 + \Delta z^2} \sqrt{I_y^2 + \Delta z^2}}$$

$$\cos\alpha_y = \frac{P_x \times I_x + \Delta z \times \Delta z}{\sqrt{P_x^2 + \Delta z^2} \sqrt{I_x^2 + \Delta z^2}}$$

where λ_x and α_x or λ_y and α_y represent the tilts around x -axis or y -axis of the pupillary axis from vertical line, λ , or of the IOL axis from pupillary axis, α . For each image, a positive angle indicates that the corresponding axis has a positive slope and vice versa for negative angles. The coordinate system is right-handed with the z -axis being the direction of propagation from the fixation target into the eye. Because the fixation target is foveal, it is assumed that the corresponding projection of the line of sight for each of the Scheimpflug images is a vertical line (ie, z -axis). Positive horizontal coordinates stand for nasal in the right eye and temporal in the left eye. Positive vertical coordinates stand for superior decentrations and negative, for inferior.

The use of 25 images from all orientations provides a more robust estimation of the IOL tilt and decentration than using only 2 images (captured at horizontal and vertical meridians). The uncertainty in tilt and decentration measurements was estimated, assuming realistic errors in edge detection and function fitting, and

an error propagation analysis was performed. These calculations predicted an accuracy of 0.2 degree for IOL tilt measurements and 0.01 mm for decentration, provided that there were no optical distortions in the original images and no additional source of error.

Physical model eye

A physical model eye in which nominal values of IOL tilt and decentration can be set was built for the study. Figure 1 shows a photograph (A) and schematic diagram (B) of the model eye. It consists of a poly(methyl methacrylate) (PMMA) water-cell model with a PMMA contact lens simulating the cornea and IOLs on a XYZ micrometer stage and rotational stage. The cornea was built by a contact lens manufacturer (AR3 Vision) with parameters similar to those of the Gullstrand eye model (corneal diameter 11.20 mm, anterior corneal radius 7.80 mm, posterior corneal radius 6.48 mm, central thickness 500 mm). Different IOLs with spherical or aspherical designs from different manufacturers (Pharmacia, Alcon, Advanced Medical Optics) and powers of 19.00 diopters (D), 22.00 D, and 26.00 D were used in place of the crystalline lens. Decentration was achieved in the horizontal direction, with a precision of 0.1 mm. Tilt of the IOL was achieved in the horizontal direction, with a precision of 0.01 degree. The anterior chamber depth could be varied, but was kept constant at 5.0 mm in this study.

Patients

Twenty-one eyes of 12 patients (mean age 72 years \pm 8 [SD]) with IOLs were measured. Time after surgery was at least 6 months. The IOLs had aspherical designs. All protocols adhered to the declaration of Helsinki and followed protocols approved by institutional review boards. All patients signed informed

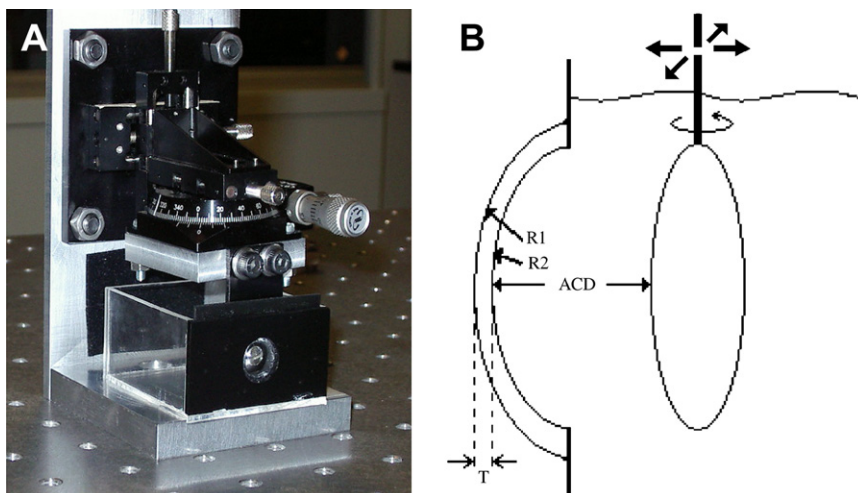


Figure 1. A: Photograph. B: Schematic diagram of the physical model eye developed for this study. A PMMA contact lens simulates the cornea ($R1 = 7.80$ mm; $R2 = 6.48$ mm; $T = 500$ mm). The IOLs are positioned with an XYZ micrometer stage and rotational stage.

consents after receiving an explanation of the purposes of the study.

Experimental protocols

The artificial eye is fixated in a translational XYZ and then aligned with the system. The main difference with respect to measurements in patients is the optical axis of the model eye is collinear with the optical axis of the instrument (as opposed to the line of sight).

Measurements were done for horizontal decentrations ranging from 0 to 2.0 mm (every 1.0 mm) and horizontal tilts (around the vertical axis) ranging from 0 to 4 degrees (every 1 degree). Because the IOL does not rotate around its own axis, decentration induced by tilt was compensated for when necessary. Alternate measurements with both the Purkinje and Scheimpflug systems were taken for each condition of tilt and decentration.

Measurements in patients were performed with pupils dilated with tropicamide 1%. In the Purkinje apparatus, patients were aligned with respect to the line of sight while they foveally viewed a fixation target presented in the minidisplay. Stabilization was achieved with a dental impression. Series of images were captured for different fixation angles (with fixation stimuli presented from -3.5 to 3.5 degrees horizontally and from -2.5 to 2.5 degrees vertically). Although only a snapshot is necessary to obtain IOL tilt and decentration, different eccentricities were tested to avoid overlapping the Purkinje images. To assess measurement reproducibility, the entire procedure was repeated 3 times. For Scheimpflug imaging, the patient foveally fixated on a fixation target. Three series of 25 images were obtained per eye.

Data processing of Purkinje imaging data requires several individual ocular biometry data to obtain coefficients A through G in the Phillips equations. For the artificial eye, these were taken from nominal values. In patients, anterior corneal radius and anterior chamber depth were measured by optical biometry (IOLMaster, Zeiss). The radii of curvature of the anterior and posterior IOL surfaces were measured using the phakometry mode of a previously described Purkinje imaging system¹⁴ if the geometry of the lens was not known.

RESULTS

Purkinje imaging and Scheimpflug raw data

Figure 2 shows typical images for the artificial eye captured with the Purkinje imaging system (*top*) and Scheimpflug camera (*bottom*), respectively. Left images correspond to an eye with a 2.0 mm decentered silicone IOL and right images to an eye with a 3.0 degree tilted acrylic IOL. Nominal decentration and tilt were set with the micrometer stages in the artificial eye. Figure 3 shows typical examples of Purkinje images (A) and Scheimpflug images (B) for 1 real eye. Differences in the diffusing properties of the real cornea and PMMA cornea of the artificial eye can be observed.

The relative positions of PI, PIII, and PIV with respect to the center of the pupil are detected from images such as those shown in Figures 2 and 3, and data are processed as explained above to obtain Purkinje tilt and decentrations. The centers of curvature of the corneal and lens surfaces and pupil center are computed from each of the 25 Scheimpflug sections, as those shown in Figures 2 and 3.

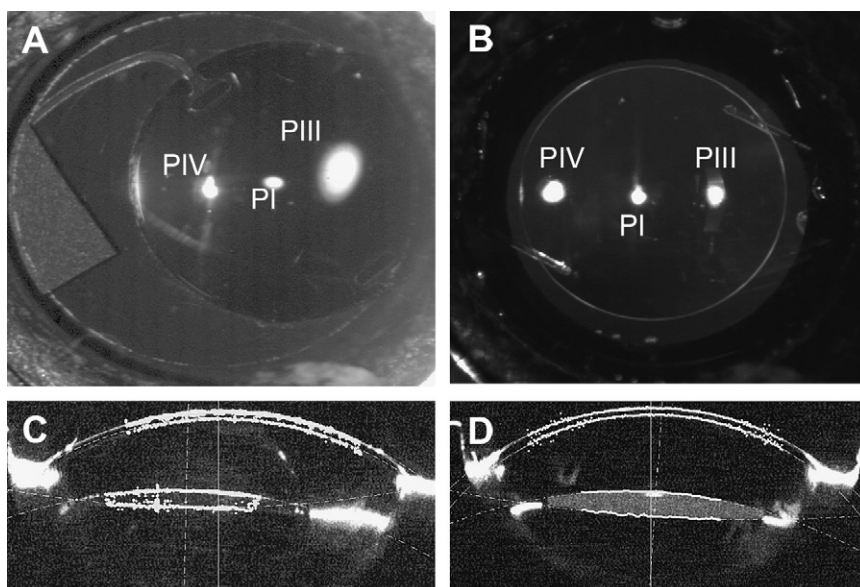


Figure 2. Raw images obtained using the Purkinje imaging system (A and B) and Scheimpflug system (C and D) from the model eye. The examples correspond to a tilted silicone IOL (B and D) and a decentered acrylic IOL (A and C). The PI, PIII, and PIV surfaces are marked on the image from the Purkinje system. The fitted curves and calculated axes are superimposed on the Scheimpflug image.

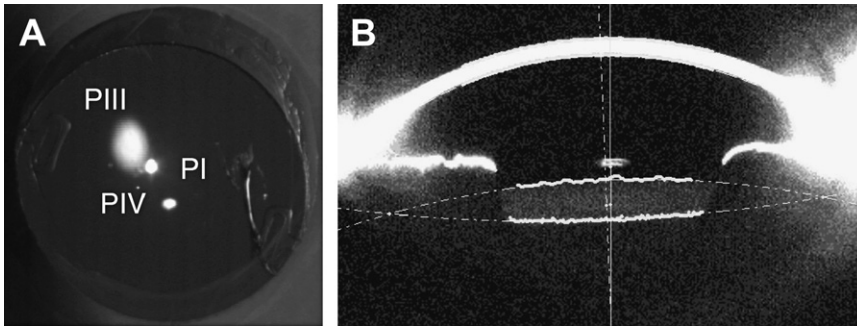


Figure 3. Raw images from the Purkinje (A) and Scheimpflug (B) systems in a real eye. As in Figure 2, the Purkinje image locations and fitted curves and the calculated axis are superimposed.

Figure 4 shows the projections of the pupillary axis, IOL axis, and decentration in 1 eye for each of the 25 meridians (with 180-degree slit rotation, from 47 to 220 degrees in right eyes and from 139 to 312 degrees in left eyes). Data are fitted to sinusoidal functions. The value of the function at 180 degrees is the x -coordinate of the IOL axis or horizontal decentration in the x -axis, and the value at 270 is the y -coordinate of the IOL axis or vertical decentration.

Tilt and decentration in the physical model eye

Figure 5 shows measured tilt from Purkinje imaging and from Scheimpflug imaging as a function of nominal tilt in the artificial eye for 3 IOLs. The solid line represents the ideal results. There was good correspondence between nominal and measured values for Purkinje imaging (mean slope 1.088; mean absolute discrepancy 0.279 degrees) and Scheimpflug imaging (mean slope 0.902; mean absolute discrepancy 0.243 degrees). Error bars represent the standard deviation of repeated measurements. Figure 5 also shows measured decentration from Purkinje imaging and from Scheimpflug imaging as a function of nominal decentration in the artificial eye for 3 IOLs. There was good correspondence between nominal and measured values for Purkinje imaging (mean slope 0.961; mean absolute discrepancy 0.094 mm) and a higher disagreement for Scheimpflug imaging (mean slope 1.216; mean absolute discrepancy 0.228 mm) when there was consistent overestimation for 2 of the measured lenses.

Tilt and decentration in patients' eyes

Figure 6 shows tilt and decentration of IOLs in right eyes and left eyes. Positive tilts around the x -axis indicate that the superior edge of the IOL is moved forward and vice versa for negative tilts around the x -axis. Positive tilts around the y -axis stand for nasal tilt and indicate that the nasal edge of the IOL is moved backward) and vice versa for a negative tilt

around the y -axis in right eyes. A positive tilt around the y -axis stands for temporal tilt (nasal edge of the IOL moves forward) in left eyes. A positive horizontal decentration stands for a nasal decentration in right eyes and temporal in left eyes, and vice versa for vertical decentration. There was clear mirror symmetry in tilt (measured with both techniques) and a less systematic trend for decentration in this group of eyes. The mean absolute tilts around the x -axis were 1.89 ± 1.00 degrees (Purkinje) and 1.17 ± 0.75 degrees (Scheimpflug), the means absolute tilts around the y -axis were 2.34 ± 0.97 degrees (Purkinje) and 1.56 ± 0.82 degrees (Scheimpflug), the mean absolute horizontal decentration was 0.34 ± 0.19 mm (Purkinje) and 0.23 ± 0.19 mm (Scheimpflug), and the mean absolute vertical decentration was 0.17 ± 0.23 mm (Purkinje) and 0.19 ± 0.20 mm (Scheimpflug). Figure 7 compares tilt and decentration measured with Scheimpflug and Purkinje imaging. The results with both techniques were highly significantly ($P < .001$) correlated for horizontal decentration ($r = 0.764$) and tilt around the y -axis ($r = 0.762$) (ie, horizontal displacements of the IOL). For vertical decentration and tilt around the x -axis, the correlations were not significant and the estimated values were close to the measurement error and method accuracy.

Repeatability of both the Purkinje and Scheimpflug methods was high: The mean standard deviation of repeated measurements was 0.61 degrees and 0.20 degrees for tilt and 0.05 mm and 0.09 mm for decentration for Purkinje and Scheimpflug, respectively. An analysis of variance for repeated measures to test whether the mean value (for each type of measurement) was representative of data found this to be the case in all conditions.

After this analysis, intraclass correlation coefficients (ICCs) were calculated to assess the reliability of the methods because the intraclass is sensitive to random error and systematic bias. The analysis showed that the methods were reliable for tilt around

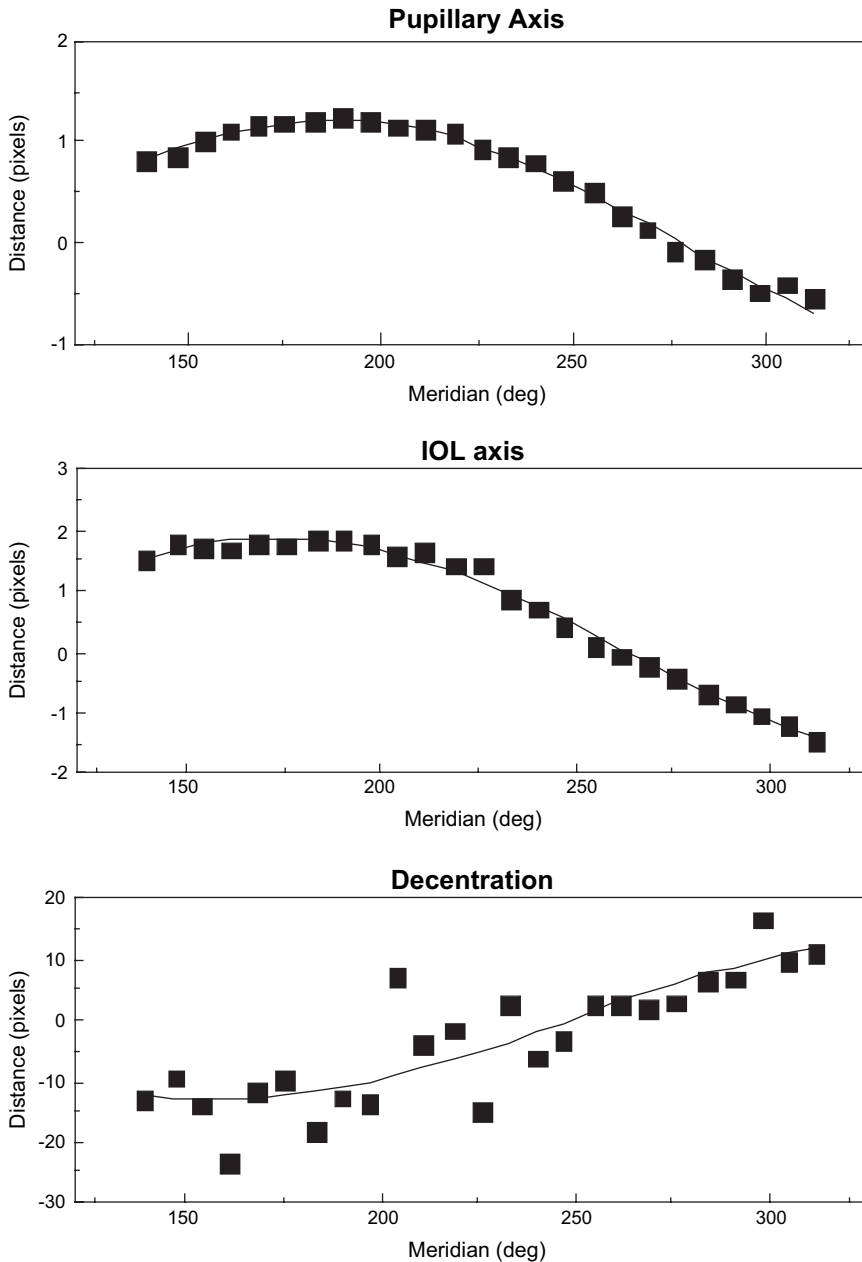


Figure 4. Pupillary axis, IOL axis location, and decentration obtained for each of the 25 images captured with the slit orientated at different meridians (indicated in the x -axis). Distances in the y -axis are indicated in pixels. For the pupillary and IOL axes, they refer to the projection of each axis to a horizontal line (difference of horizontal values between 2 arbitrary Z positions; here $Z = 0$ pixels and $Z = 20$ pixels). For decentration, they refer to the distance between IOL center and pupillary axis. The data (ie, projections for each orientation) are fit to a sinusoidal function, shown by a solid line. The fit of the decentration is slightly noisier because of the tilt of the reference axis. The horizontal and vertical coordinates of each axis, IOL tilt (degrees), and the decentration (mm) are calculated from those data, as explained in the text.

the y -axis (ICC 0.830) and decentration in the x -axis (ICC 0.836).

DISCUSSION

Limitations of the techniques

The Purkinje imaging system has been extensively validated computationally and experimentally in previous studies.^{14,15} Computer simulations using eye models and the actual optical configuration of the system show that deviations from spherical model eyes resulting from corneal asphericity or corneal irregularities and anterior and posterior lens surfaces

asphericities did not significantly affect the results of IOL tilt and decentration.

Scheimpflug images from the Pentacam system are not corrected for optical distortion, and the CCD images also suffer from geometric distortion. The former is corrected by software at the corneal level, but not at the crystalline lens or IOL levels. The second can be compensated for using calibration grids. This is implemented in the commercial software to provide corrected biometry values, and we developed a routine to compensate for the raw images. The presence of uncorrected distortions induces errors that must be studied. We compared the measured values of tilt and

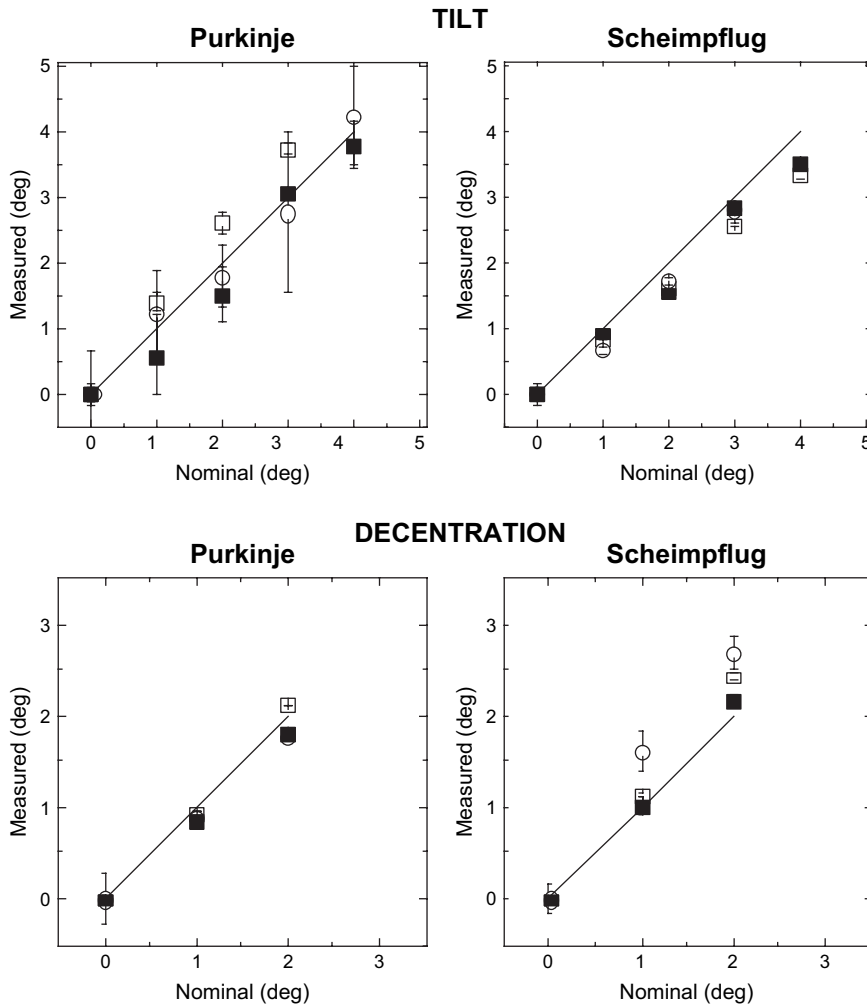


Figure 5. Experimental IOL tilt and decentration for the model eye for 3 different lenses (plotted with different symbols) as a function of nominal values of tilt and decentration. Nominal tilt ranged from 0 to 4 degrees and nominal decentration ranged from 0 to 2 mm. The ideal $X = Y$ line has also been plotted.

decentration in the physical model eye with and without compensation for geometric distortion. When processing the data of Figure 5 without correcting geometrical distortion, we found a constant underestimation of tilt for all IOLs (mean slope 0.866; mean discrepancy 0.280 degrees) and higher overestimation of decentration (mean slope 1.233; mean discrepancy 0.247 mm).

In addition, we performed control experiments to evaluate the possible effect of optical distortion on tilt and decentration measurements with the Scheimpflug system. Using the same physical model eye, we performed measurements in which the spherical cornea was replaced by flat surfaces as well as experiments with and without water in the cell. These different configurations necessarily change the contributions of the optical distortion. Figure 8, shows nominal versus measured tilts (as in Figure 5, now for the different physical model eye settings). In general, the refractive powers in front of the lens did not affect tilt measurement. Correlations of nominal versus

experimental values show slopes of 0.849 for the spherical cornea with water, 1.015 for the spherical cornea without water, 0.883 for the flat cornea without water, and 0.968 for the lens alone without a cornea. We conducted similar control experiments for decentered lenses. We found slopes of 1.0530, 0.888, 0.927, and 1.025, respectively. This shows that optical distortions have only a moderate influence on the measurement of tilt and decentration.

Our measurements with both techniques showed high reproducibility. The Purkinje imaging system has limitations when lenses are very flat, for which PIII is quite large. The system also relies on the appropriate measurement of the anterior and posterior lens radii of curvature. Scheimpflug imaging requires sufficient pupil dilation to visualize the posterior lens surface and collaboration from the patients to fixate for 1.5 seconds without moving while illuminated with a blue light (versus 30 exposure time and IR illumination with the Purkinje imaging system). Scheimpflug imaging also poses some challenges

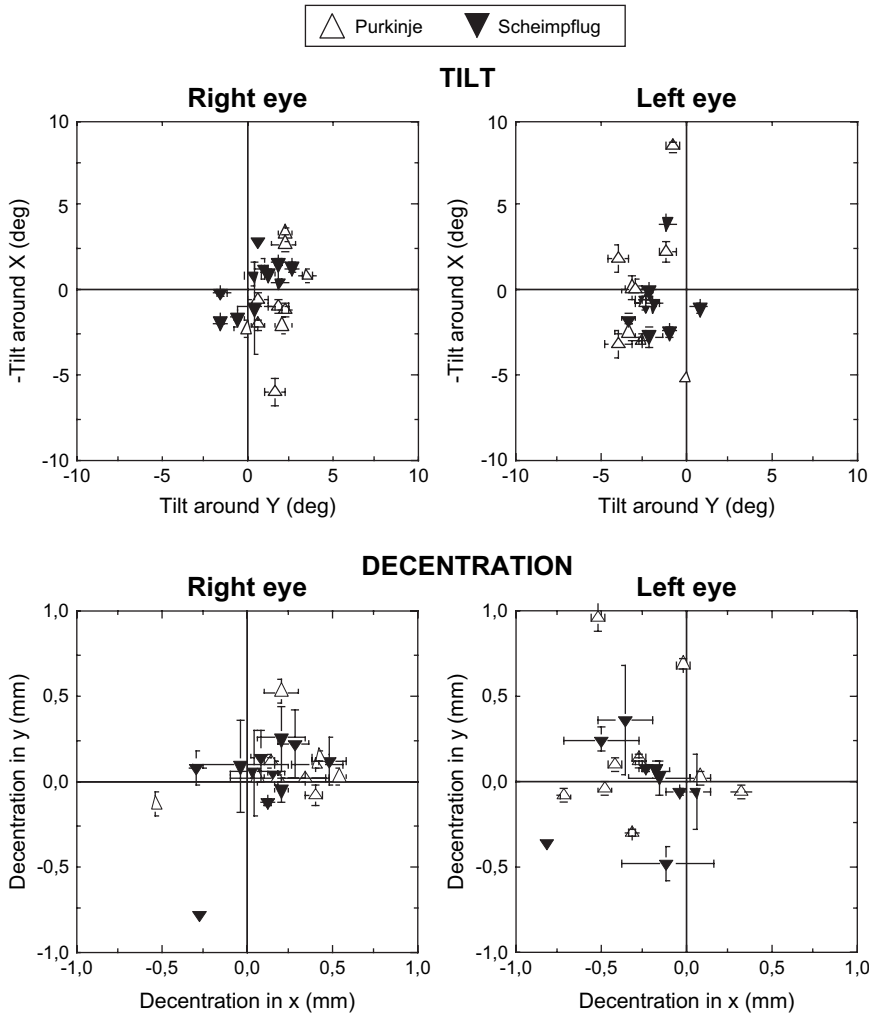


Figure 6. Tilt and decentration in right eyes and left eyes of patients using Purkinje (*open symbols*) and Scheimpflug (*solid symbols*) imaging. Refer to the text for details on sign conventions. The sign of the tilt around *x*-axis was changed to allow a more graphic representation of lens positioning, assuming a frontal view of the patients' eyes.

with low-diffusing IOLs. Optical and geometrical distortion of the Scheimpflug images (obtained directly from the CCD) produce slight discrepancies of the measured tilt and decentration, which improve with the correction of the geometrical distortion.

In real eyes, in general, both techniques agreed well for horizontal IOL tilt and decentration. The larger discrepancies, particularly for vertical decentration, may be attributed to small magnitudes found close to the nominal accuracy of the techniques.

Comparisons with previous studies and implications

In this study, we present experimental validation of a previously presented Purkinje imaging system to measure IOL tilt and decentration using a physical model eye. We also proposed a new robust method to calculate IOL tilt and decentration using a commercial Scheimpflug imaging system, which is validated using the same physical model eye. A comparison of

tilt and decentration measurements in real eyes using both techniques is also presented.

Purkinje and Scheimpflug methods have been used before to measure IOL tilt and decentration. To our knowledge, only the reports of Barry et al.¹³ and Rosales and Marcos¹⁴ were based on thoroughly validated Purkinje imaging methods. Several studies report tilt and decentration measured with Scheimpflug imaging, in most cases from 2 sections of the anterior segment captured at perpendicular meridians. Coopens et al.,²⁹ working with a modified Nidek system, used 2 or more images to create a redundant data set to check the procedure. In the present study, we used combined information from 25 meridians. To our knowledge, only Coopens et al. corrected the Scheimpflug images for geometric and optical distortion to measure IOL tilt and decentration. We have found that not correcting for geometric distortion causes slightly discrepancies in the measured values.

We found mean Scheimpflug and Purkinje values of 0.21 ± 0.28 mm horizontally and 0.03 ± 0.38 mm

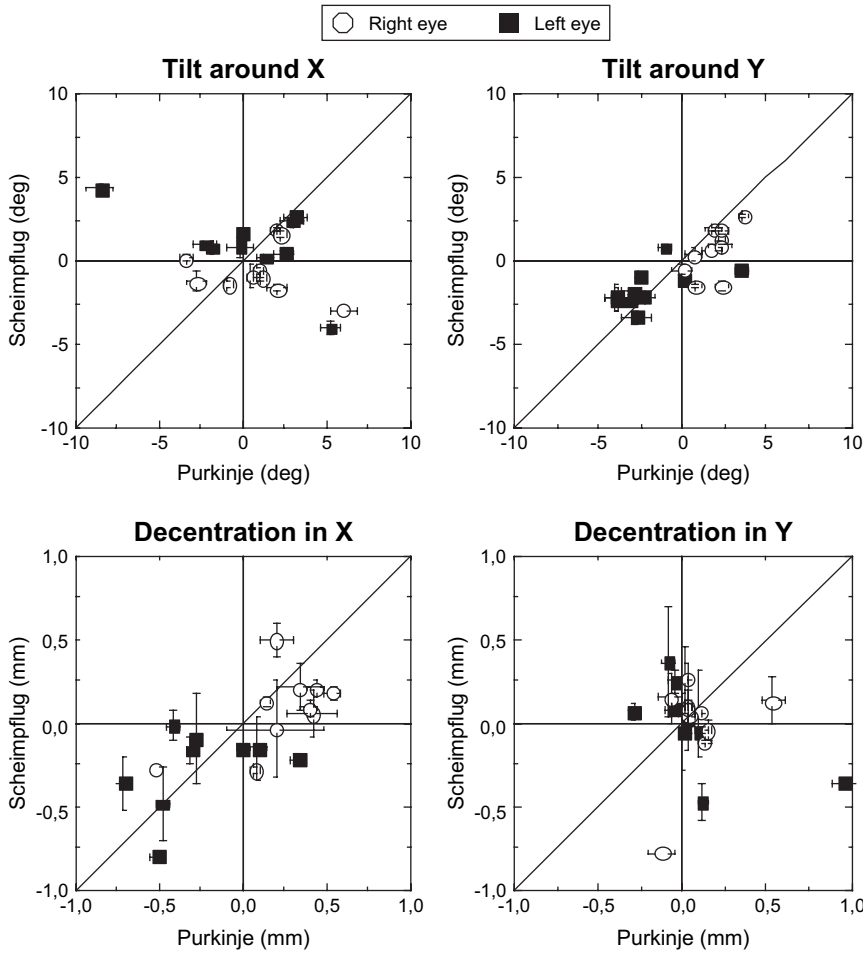


Figure 7. Comparison of the horizontal and vertical components of IOL tilt and decentration between Scheimpflug and Purkinje techniques. The ideal X = Y line is also shown.

vertically for decentration and -0.26 ± 2.63 degrees around the x -axis and 1.54 ± 1.50 around the y -axis for tilt. Decentrations in x -axis and tilts around the y -axis were nasal in both eyes. In general, the amounts

of tilt and decentration we report are lower than those of the earliest reports in the literature. For example, Phillips et al.¹² report a mean decentration of 0.7 ± 0.3 mm and mean tilt of 7.3 ± 3.0 degrees without

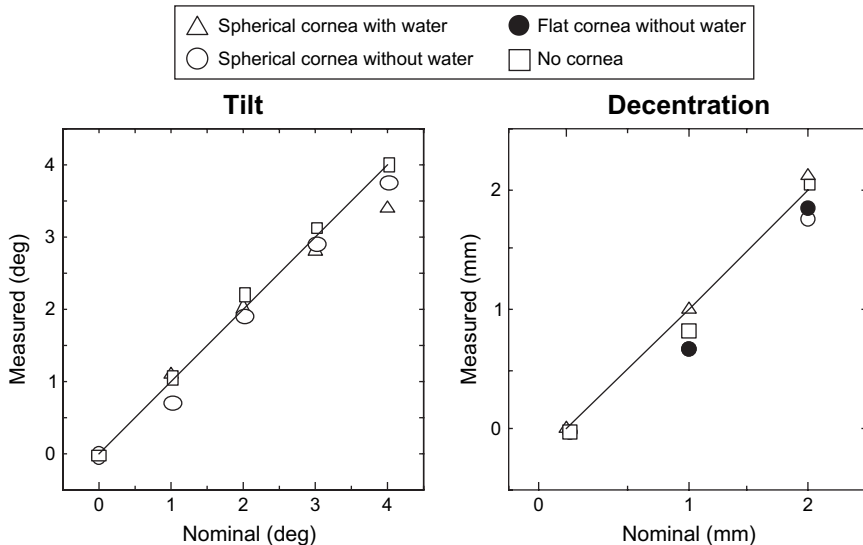


Figure 8. Nominal versus experimental tilt and decentration in the physical model eye for a set of conditions, aiming at assessing the influence of optical distortion on the tilt and decentration estimated from Scheimpflug images. Each symbol represents a different condition (flat or curved “cornea,” with or without water, isolated lens). Tilt and decentration in these control experiments were set as in the experiments in Figure 5.

specifying the direction of tilt or decentration. One report of IOL position after transscleral implantation found systematically high amounts of tilt and decentration (mean 5.97 ± 3.68 degrees and 0.63 ± 0.43 degrees, respectively), which the authors attribute to the implantation technique.³¹ Our results are more comparable with those in more recent studies, reporting lower tilt and decentration values, and are probably associated with an improvement in surgical procedures. Previous results with our Purkinje imaging system of measurement of IOL tilt and decentration¹⁴ showed a mean tilt of 0.87 ± 2.16 degrees around the *x*-axis and 2.3 ± 2.33 degrees around the *y*-axis; mean horizontal decentration was 0.25 ± 0.28 mm and mean vertical decentration, -0.41 ± 0.39 mm.

Other studies using noncorrected Scheimpflug images report mean tilts between 2.61 ± 0.84 degrees (3-piece acrylic IOLs²²) and 3.4 ± 2.02 degrees (silicone IOLs²⁷) and mean decentrations of 0.29 ± 0.26 mm to 0.37 ± 0.19 .²² To our knowledge, only 1 study mentions interocular mirror symmetry for tilt and decentration with phakic IOLs.²⁹ Although most studies and techniques provide similar mean values that agree well with the mean values reported here using both Purkinje and Scheimpflug, we have shown that in individual patients, some discrepancies across techniques may be found. This is particularly important when using Scheimpflug images that have not been corrected for geometric and optical distortion, as in the raw images provided by commercially available instruments such as the Pentacam.

Finally, the amounts of tilt and decentration found in patients were in general low, and particularly for the decentration were of the order of the resolution of the techniques in many patients. The clinical relevance of tilt and decentration of these amounts is likely limited, although there are case reports in the literature in which they resulted in decreased visual function (Rosales P, et al. IOVS 2006; 47:ARVO E-Abstract 313).³²

REFERENCES

- Bellucci R. Multifocal intraocular lenses. *Curr Opin Ophthalmol* 2005; 16:33–37
- Dick HB. Accommodative intraocular lenses: current status. *Curr Opin Ophthalmol* 2005; 16:8–26
- Moreno-Barriuso E, Merayo-Llodes J, Marcos S, et al. Ocular aberrations before and after myopic corneal refractive surgery: LASIK-induced changes measured with laser ray tracing. *Invest Ophthalmol Vis Sci* 2001; 42:1396–1403
- Barbero S, Marcos S, Jiménez-Alfaro I. Optical aberrations of intraocular lenses measured in vivo and in vitro. *J Opt Soc Am A Opt Image Sci Vis* 2003; 20:1841–1851
- Marcos S, Barbero S, Jiménez-Alfaro I. Optical quality and depth-of-field of eyes implanted with spherical and aspheric intraocular lenses. *J Refract Surg* 2004; 21:223–235
- Holladay JT, Piers PA, Koranyi G, et al. A new intraocular lens design to reduce spherical aberration of pseudophakic eyes. *J Refract Surg* 2002; 18:683–691
- Altmann GE. Wavefront-customized intraocular lenses. *Curr Opin Ophthalmol* 2004; 15:358–364
- Atchison DA. Design of aspheric intraocular lenses. *Ophthalmic Physiol Opt* 1991; 11:137–146
- Dunne MCM, Davies LN, Mallen EAH, et al. Non-invasive phakometric measurement of corneal and crystalline lens alignment in human eyes. *Ophthalmic Physiol Opt* 2005; 25: 143–152
- Kirschkamp T, Dunne M, Barry J-C. Phakometric measurement of ocular surface radii of curvature, axial separations and alignment in relaxed and accommodated human eyes. *Ophthalmic Physiol Opt* 2004; 24:65–73
- Auran JD, Koester CJ, Donn A. In vivo measurement of posterior chamber intraocular lens decentration and tilt. *Arch Ophthalmol* 1990; 108:75–79
- Phillips P, Pérez-Emmanuelli J, Rosskothén HD, Koester CJ. Measurement of intraocular lens decentration and tilt in vivo. *J Cataract Refract Surg* 1988; 14:129–135
- Barry J-C, Dunne M, Kirschkamp T. Phakometric measurement of ocular surface radius of curvature and alignment: evaluation of method with physical model eyes. *Ophthalmic Physiol Opt* 2001; 21:450–460
- Rosales P, Marcos S. Phakometry and lens tilt and decentration using a custom-developed Purkinje imaging apparatus: validation and measurements. *J Opt Soc Am A Opt Image Sci Vis* 2006; 23:509–520
- Rosales P, Dubbelman M, Marcos S, van der Heijde R. Crystalline lens radii of curvature from Purkinje and Scheimpflug imaging. *J Vision* 2006; 6:1057–1067
- Dubbelman M, van der Heijde GL. The shape of the aging human lens: curvature, equivalent refractive index and the lens paradox. *Vision Res* 2001; 41:1867–1877
- Lapuerta P, Schein SJ. A four-surface schematic eye of macaque monkey obtained by an optical method. *Vision Res* 1995; 35:2245–2254
- Brown N. Slit-image photography and measurement of the eye. *Med Biol Illus* 1973; 23:192–203
- Koretz JF, Cook CA, Kaufman PL. Accommodation and presbyopia in the human eye: changes in the anterior segment and crystalline lens with focus. *Invest Ophthalmol Vis Sci* 1997; 38:569–578
- Dubbelman M, van der Heijde GL, Weeber HA. Change in shape of the aging human crystalline lens with accommodation. *Vision Res* 2005; 45:117–132
- Koretz JF, Strenk SA, Strenk LM, Semmlow JL. Scheimpflug and high-resolution magnetic resonance imaging of the anterior segment: a comparative study. *J Opt Soc Am A Opt Image Sci Vis* 2004; 21:346–354
- Wang M-C, Woung L-C, Hu C-Y, Kuo H-C. Position of poly (methyl methacrylate) and silicone intraocular lenses after phacoemulsification. *J Cataract Refract Surg* 1998; 24: 1652–1657
- Sasaki K, Sakamoto Y, Shibata T, et al. Measurement of postoperative intraocular lens tilting and decentration using Scheimpflug images. *J Cataract Refract Surg* 1989; 15:454–457
- Baumeister M, Neidhardt B, Strobel J, Kohnen T. Tilt and decentration of three-piece foldable high-refractive silicone and hydrophobic acrylic intraocular lenses with 6-mm optics in an intraindividual comparison. *Am J Ophthalmol* 2005; 140: 1051–1058
- Hayashi K, Hayashi H, Nakao F, Hayashi F. Comparison of decentration and tilt between one piece and three piece polymethyl

- methacrylate intraocular lenses. *Br J Ophthalmol* 1998; 82: 419–422
26. Jung CK, Chung SK, Baek NH. Decentration and tilt: silicone multifocal versus acrylic soft intraocular lenses. *J Cataract Refract Surg* 2000; 26:582–585
27. Kim JS, Shyn KH. Biometry of 3 types of intraocular lenses using Scheimpflug photography. *J Cataract Refract Surg* 2001; 27:533–536
28. Nejima R, Miyata K, Honbou M, et al. A prospective, randomised comparison of single and three piece acrylic foldable intraocular lenses. *Br J Ophthalmol* 2004; 88:746–749
29. Coopens JE, van den Berg TJTP, Budo CJ. Biometry of phakic intraocular lens using Scheimpflug photography. *J Cataract Refract Surg* 2005; 31:1904–1914
30. Atchison DA, Smith G. *Optics of the Human Eye*. Oxford, England, Butterworth-Heinemann, 2000
31. Durak I, Öner HF, Koçak N, Kaynak S. Tilt and decentration after primary and secondary transsclerally sutured posterior chamber intraocular lens implantation. *J Cataract Refract Surg* 2001; 27:227–232
32. Oshika T, Kawana K, Hiraoka T, et al. Ocular higher-order wavefront aberration caused by major tilting of intraocular lens. *Am J Ophthalmol* 2005; 140:744–746



First author:
Alberto de Castro, BSc